Available online at www.sciencedirect.com

ScienceDirect

Procedia Structural Integrity 2 (2016) 144–151

Structural Integrity
Procedia

www.elsevier.com/locate/procedia

21st European Conference on Fracture, ECF21, 20-24 June 2016, Catania, Italy

A Method to Improve the Fracture Toughness Using 3D Printing by Extrusion Deposition

Julien Gardan[a,b]*, Ali Makke[a,b], Naman Recho[a,c]

[a] *EPF, Engineering school, 2 rue Fernand Sastre, Troyes, France*
[b] *Institut Charles Delaunay, LASMIS, UTT,UMR CNRS 6281, 12 rue Marie Curie, 10010 Troyes, France*
[c] *Pascal Intitute, Blaise Pascal University, 63000 Clermont Ferrand, France*

Abstract

Additive manufacturing or 3D printing have strongly been developed the last years and currently propose several solutions. Fused Deposition Modeling (FDM) is a layer additive manufacturing process that uses a thermoplastic filament by fused deposition which builds its geometry along trajectories generated by slicing. This process leads to a locally heterogeneous structure because of the weld lines between the deposed threads. These trajectories (and then the weld lines) are predefined and not necessarily based on the specific mechanical constraints from product's use. As a consequence, the weld lines can be found oriented in bad directions that reduce the mechanical strength of the printed sample. In this work we used finite elements simulation to identify the principal directions of the stress in a standard Crack Test C-T sample. The aim is to reproduce the principal stress directions inside the internal structure of cracking sample realized in extrusion deposition by 3D printing in order to improve the fracture toughness. Several samples made from Acrylonitrile-Butadiene-Styrene were printed and tested. We analyze the outcomes by comparing a C-T standard tensile test procedure with classical and optimized filament depositions. The tests show improved mechanical characteristics and thus provide a method to deposit a filament along a trajectory adapted to the mechanical stresses. Crack branching is observed through a heterogeneous structure and then discussed. On the basis of these results, the cracked specimen will define a new strategy to reinforce the specimen by a specific fused deposit lines.

Keywords: Additive Manufacturing; 3D Printing; Crack stress field; Fracture resistance; Fracture type; Crack extension.

---

* Corresponding author. Tel.: +33 (0)1 41 13 48 97
E-mail address: julien.gardan@epf.fr

10.1016/j.prostr.2016.06.019

1. Introduction

Additive Manufacturing (AM) area involves many technologies which are able to produce of complex geometries by layers manufacturing. Those technologies depend on material and its hardening system like the sintering or melting by laser, the binder or resin jetting, or the filament depositing (Gardan, 2015). From one technology to another, the manufacture direction, the model orientation and the material behavior are important to get an accurate model and an efficient production (Beaman et al., 1997). Fused Deposition Modeling (FDM) is a layer additive manufacturing process that uses a thermoplastic filament by fused deposition which builds its geometry along trajectories generated by slicing. This technology is close to numerical control machine with three axes and originally uses a programming language G-code. Then, 3D printer manufacturers have converted this code in proprietary format for their machines. Through this depositing, the filament trajectory is defined to fill the product and also create a shell with often a stripe shape at 45° by alternate layers.

This process leads to a locally heterogeneous structure because of the weld lines between the deposed threads. These trajectories are predefined and not essentially based on the specific mechanical constraints from product's use. As a consequence, the weld lines can be found oriented in bad directions that reduce the mechanical strength of the printed sample. In order to apply a depositing trajectory able to take an account the mechanical behavior of product, this study tackles the generating a filament trajectory coupled to localized stresses of a product. In this work, authors used finite elements simulation to identify the principal directions of the stress in a standard Crack Test C-T sample. The aim is to reproduce the principal stress directions inside the internal structure of cracking sample realized in extrusion deposition by 3D printing in order to improve the fracture toughness.

Several samples made from Acrylonitrile-Butadiene-Styrene were printed and tested. The approach analyzes the outcomes by comparing a C-T standard tensile test procedure with classical and optimized filament depositions. The tests show improved mechanical characteristics and thus provide a method to deposit a filament along a trajectory adapted to the mechanical stresses. Crack branching is observed through a heterogeneous structure and then discussed. On the basis of these results, the cracked specimen will define a new strategy to reinforce the specimen by a specific fused deposit lines.

2. Fused Depositing Modeling

Fused Depositing Modeling (FDM) process begins with a 3D model in CAD or modeling software before converting it in STL format file. This format is treated by specific software own to the AM technology which cuts the piece in slices to get a new file containing the information for each layer. This step implies a G-code language to traduce the slicing in trajectories and layers. During the manufacturing, a filament is extruded through a nozzle to print one cross section of an object, then moving up vertically to repeat the process for a new layer (Fig. 1). The most used materials in FDM are ABS, PLA, and PC (Polycarbonate). To predict the mechanical behavior of FDM parts, it is critical to understand the material properties of the raw FDM process material, and the effect that FDM build parameters have on anisotropic material properties (Ahn et al., 2002). The first desktop 3D printers like the fab@home were linked at open source software which proposed other thread depositing strategies (Malone and Lipson, 2007). About the internal structures of products realized by 3D Printing, some studies like (Vesenjak et al., 2010) investigate the use of lattice structures including rapid prototyping to lighten sandwich panels while maintaining their mechanical strength. The study enabled to determine that the directions of the anisotropy of the lattice influences the mechanical behaviour of the entire panel used. The lattice modelling can be adjusted according to the specifications of mechanical strength. Other studies develop specific structures like curved (Galantucci et al., 2008), honeycomb (Abramovitch et al., 2010) or cell shapes, "tetrachirales" (Miller et al., 2010) or "hexachirales" (Prall and Lakes, 1997). The use of a thread deposition more suited to mechanical constraints of product according to its use has not been more explored.

The support material is often made of another material and is removable or soluble from the actual part at the end of the manufacturing process (except for the low cost solutions, which use the same raw material). FDM technology is the most popular of desktop 3D printers and the less expensive professional printers. The FDM technology was invented in the 1980s by Scott Crump (Crump, 1992, 1994).

In this study, authors use a Makerbot Replicator 3D printer to manufacture the specimens in ABS (Acrylonitrile-Butadiene-Styrene) material.

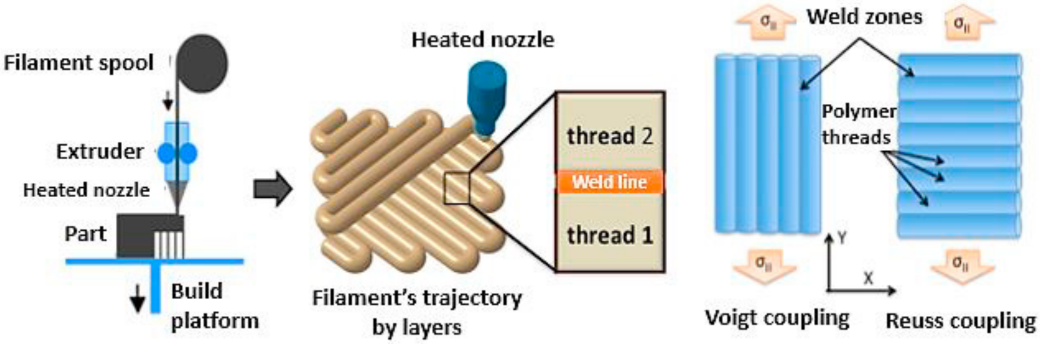

Fig. 1. Fused Depositing Modeling (FDM) and classical trajectory deposition

3. Simulation and depositing approach

The research defined an approach, which matches a numerical simulation phase and a depositing fabrication phase in order to realize standard samples. The filament trajectory from depositing by 3D Printing is used to reproduce the principal directions of the stress from finite elements simulation of standard Crack Test C-T sample.

The Figure 2 below illustrates the research approach with different steps. The process begins with the geometry model in order to compute the mechanical stresses through the numerical simulation. Then, the 3D model is modified to specify the limit of principal directions according to the stress fields. The product slicing is realized with open source softwares (Slic3r v 1.2.6 and Replicator G) but the G-code and the alternate layers reproducing the stress fields are processed manually into the programming language. Finally, the samples are manufactured by 3D printing in filament depositing and the study tackles the mechanical tests in order to find the fracture toughness with the samples improvement. In the next section, the paper describes the generative trajectory from the finite element simulation.

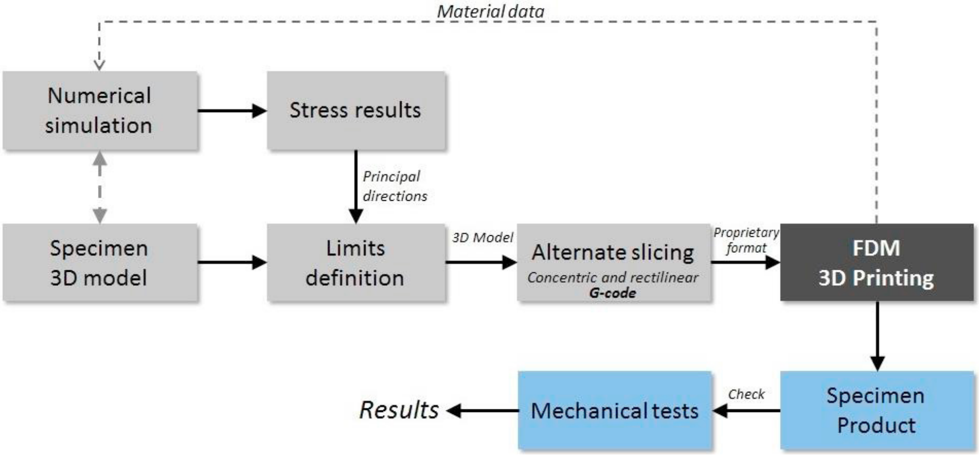

Fig. 2. Research process

4. Numerical simulation

Finite Elements (FE) simulation of a linear elastic model has been used to compute the principal stresses and strains in the sample with plane stress conditions. The principal stresses σ_I and σ_{II}, which are the eigenvalues of the stress tensor, can be written as:

$$\sigma_I = \frac{\sigma_{11}+\sigma_{22}}{2} + \sqrt{\left(\frac{\sigma_{11}+\sigma_{22}}{2}\right)^2 + {\sigma_{12}}^2} \qquad (1)$$

$$\sigma_{II} = \frac{\sigma_{11}+\sigma_{22}}{2} - \sqrt{\left(\frac{\sigma_{11}+\sigma_{22}}{2}\right)^2 + {\sigma_{12}}^2} \qquad (2)$$

σ_{ij} are the component of the stress tensor.
The principal directions, which are the eigenvectors of the stress tensor, can be described by the angle θ where

$$\tan(2\theta) = \frac{2\sigma_{12}}{\sigma_{11} - \sigma_{22}} \qquad (3)$$

The printed specimen used for fracture toughness characterization is a standard Crack Test (CT) sample. The specimen thickness is about 6,5mm, thus plane stress assumption is almost verified. We should note that the printed material is considered as homogenous at the first step of the FE analysis.

4.1. Stress concentration region

Generally speaking, to improve the mechanical properties of a printed sample, the polymer threads must be oriented toward the tensile force field (or traction stress) in the sample. This idea is inspired from the reinforcement principle of the composite materials where the fibers are oriented toward the in-plane tensile stress.

Figure 3 describes the strong and the weak configuration of the deposit threads. The Voigt coupling between threads leads to a strong configuration when tensile stress is encountered. For this reason the geometry of the sample to be printed is divided into two domains.

(i) The stress concentration vicinity (around geometric singularities, holes…)
(ii) The rest of the sample where the stress magnitude is not significantly high.

The stress concentration vicinity is the most critical region in the sample because of the high Von Mises stress inside. This region should be printed carefully in order to avoid the weak configuration of threads. According to the strategy of thread deposit optimization, the improvement of the mechanical properties is expected where the principal stresses are mainly tensile (both σ_I and σ_{II} are positives). This fact helps us to define the region where the modification of extrusion trajectory is beneficial. This region called hereafter the “affected region” Ω_1 is defined as follow:
If Ω is the entire geometry of the sample and M is a random point within this geometry then:

$$\Omega = \Omega_1 \cup \Omega_2$$

$$\forall M \in \Omega \;\; if \;\; \begin{cases} (\sigma_I > 0)\,\&\&\,(\sigma_{II} > 0) \;\rightarrow\; M \in \Omega_1 \\ else \;\rightarrow\; M \in \Omega_2 \end{cases}$$

Figure 3(a) shows the affected region in a standard CT sample.
The optimization of the thread deposit trajectories will be performed only within the region that is defined upon this criterion.

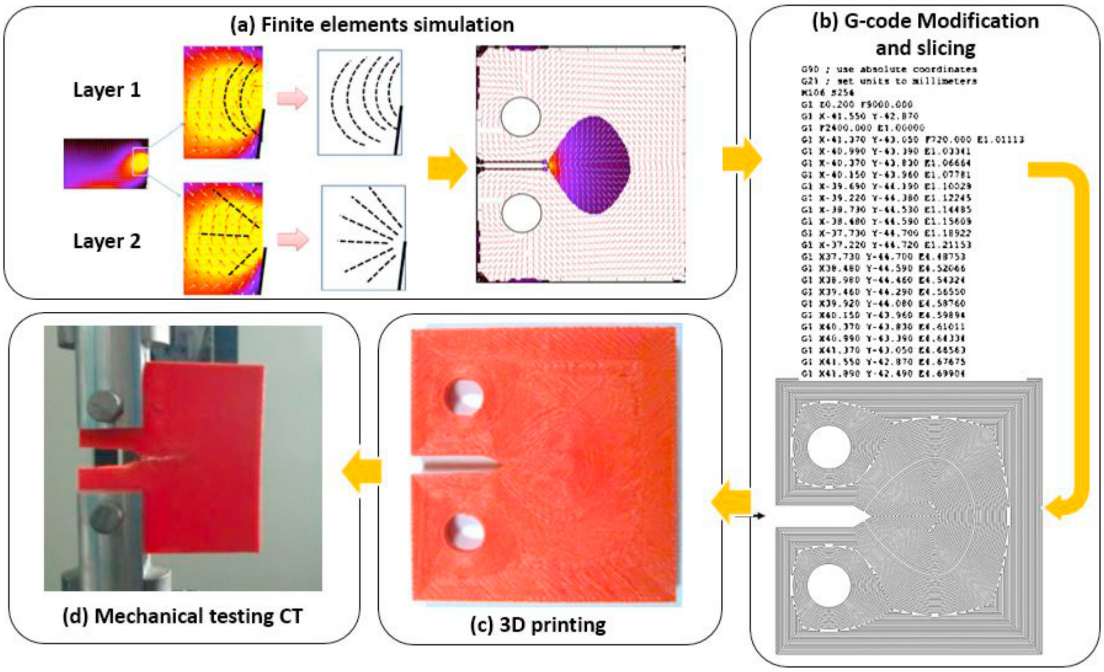

```
G90 ; use absolute coordinates
G21 ; set units to millimeters
M106 S254
G1 Z0.200 F9000.000
G1 X-41.550 Y-42.870
G1 F2400.000 E1.00000
G1 X-41.370 Y-43.050 F720.000 E1.01113
G1 X-40.990 Y-43.390 E1.03341
G1 X-40.370 Y-43.830 E1.06664
G1 X-40.150 Y-43.960 E1.07781
G1 X-39.690 Y-44.190 E1.10029
G1 X-39.220 Y-44.380 E1.12245
G1 X-38.730 Y-44.530 E1.14485
G1 X-38.480 Y-44.590 E1.15609
G1 X-37.730 Y-44.700 E1.18922
G1 X-37.220 Y-44.720 E1.21153
G1 X37.730 Y-44.700 E4.48753
G1 X38.480 Y-44.590 E4.52066
G1 X38.980 Y-44.460 E4.54324
G1 X39.460 Y-44.290 E4.56550
G1 X39.920 Y-44.080 E4.58760
G1 X40.150 Y-43.960 E4.59894
G1 X40.370 Y-43.830 E4.61011
G1 X40.990 Y-43.390 E4.64334
G1 X41.370 Y-43.050 E4.66563
G1 X41.550 Y-42.870 E4.67675
G1 X41.890 Y-42.490 E4.69904
```

Fig. 3. Depositing trajectory according to principal directions

4.2. Printing Trajectories

The principal directions are computed as described above at each point in the sample. These directions (eigenvectors) are tangent to the printing trajectory. As the in-plane stress is biaxial then there are two principal directions in the sample. As a consequence, two trajectories are to be taken into account in the printing. For this reason, the thickness dimension of the sample is built by alternate layers. For two subsequent layers, the first (second) principal direction is used to calculate the trajectory in the first (second) layer as shown in Fig. 3 (b).

5. 3D printing of samples

5.1. Generative trajectory of 3D printing

The slicing of 3D Model (.stl) is applied with concentric fill pattern around the delimited zone according to the crack simulation. The printing trajectory must agree with the principal direction in the delimited zone (Fig. 3). The other “white” domain is less stressed (in the tensile direction) and is printed without respecting the principal direction conditions. The G-code is modified to alternate the layers with the principal direction and the less stressed direction. The depositing trajectory shows a drawing of the thread close to stress fields’ results.

5.2. Samples manufacturing

In order to compare classical and optimized samples, two types of standard Crack Test C-T samples are printed. The first “classical” sample is got by linear infilling with 45 degree depositing by alternate layers and the second “optimized” sample uses the previous generative trajectory method (Fig 4.).

6. Cracking test with C-T samples

6.1. Conditions

The tests procedure was used with the Crack Test C-T samples fabricated with the ‘MakerBot’ Replicator. A tensile test machine Instron 4484 was used to carry out uniaxial tensile tests with specific tensile tool for the Crack Tests adapted to specimens (Fig. 4.). The displacement speed of the machine was 1mm.min-1 with a sampling period of 500m.s-1. The load cell capability is 150 KN and the procedure used three (3) samples for “classical” and “optimized” models.

6.2. Cracking tests

After the cracking tests, the results show fracture propagation from the notch to observe some crack extension. The “classical” samples have a straight fracture due to alternating layers with a thread deposit at 45°. The “optimized" samples have a dendritic fracture with a dispersion of the stress field localized into the zone which reproduces the principal directions in order to resist to the propagation.

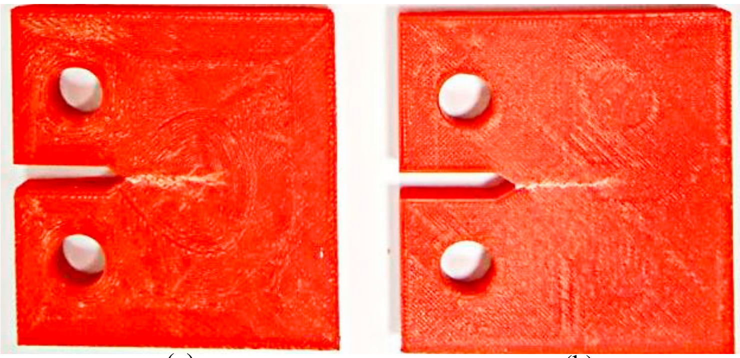

(a) (b)

Fig. 4. Crack extension: optimized samples (a) and classical (non-optimized) samples (b)

6.3. Results and discussion

Figure 5 compares the force/displacement curves for tested CT samples. The Numeric values of the maximum force and its corresponding displacement are shown in the tables 1 and 2. Two CT specimens relative to these tests are shown in figure 4.

According to these curves, there are two mains improvements to be highlighted regarding (i) the maximum force reached in the test and (ii) the ultimate displacement.

(i) For the not-optimized samples, the maximum tensile load doesn’t rise above 1410 N, whereas it reaches 1743 N for the optimized samples. We have also found that the average of the maximum fracture force for optimized samples is always higher than the not-optimized one. The optimized samples are clearly stronger than the classical samples through an adequate printing.

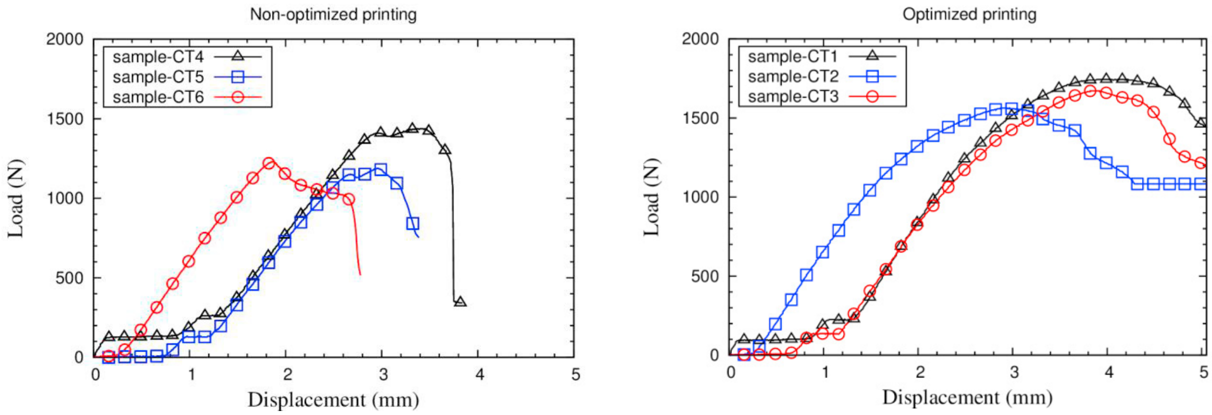

Fig. 5. Fracture test results, comparison between the non-optimized printing results (left) and the optimized printing results (right).

The results are compared into the *table 1* and the *table 2* with the average of mechanical behavior of three ABS samples used into a FDM 3D printer in order to positioning the data.

Table 1. Mechanical results of optimized samples

Optimized type	Maximum applied force to Fracture (N)	Displacement (*mm*)
Sample C-T 1	1743,57	4,22
Sample C-T 2	1562,36	2,94
Sample C-T 3	1671,09	3,92
Average	1659,00	3,69

Table 2. Mechanical results of classical samples

Classical type	Maximum applied force to Fracture (N)	Displacement (*mm*)
Sample C-T 4	1409,35	2,99
Sample C-T 5	1187,88	2,95
Sample C-T 6	1232,15	1,87
Average	1276,46	2,60

The optimized C-T samples have higher fracture strength up to 20% than classical samples.

(ii) The maximum displacement of the grips just before the ultimate failure reaches 3.8 mm for the not-optimized samples, while it is always greater than 5mm for the optimized samples. The increase of the displacement lies on the crack propagation mechanism in the structure. The crack propagation mechanisms was found strongly affected by the filament orientation in the sample, as explained below. It's to be noted that more tests are needed in order to control the scatter observed in various samples.

Another observation can be highlighted regarding the crack extension path. Figure 4 shows clearly that the crack path in the classical sample is almost a straight line while in the optimized sample the crack has a dendritic aspect because of the ramifications behind the main crack. This behavior has been also observed for the other four samples (not shown here). As the crack test is performed under quasi statics tensile conditions then there are no dynamic effects related to the observed branching. In fact, this behavior arises from the local structure of the material around the crack tip, and how the weld lines are distributed in this vicinity. In the optimized samples the cracks begins at the sample notch as expected. At the beginning of the extension, the crack is typically in mode 1 (tensile). After that, the crack is deviated by a weld line, then it becomes a mixed mode crack (tensile + shear). The shear stress near to the crack tip leads to a strain hardening then the material strength increases locally. The crack in the ramification is stopped and the main crack returns to mode I and continues from its main initial path.

This behavior seems to be related to the improvement in the fracture toughness observed for optimized printed sample. The local shear flow in the ramification vicinity contributes to energy dissipation of the crack, this delays the crack extension in the sample and improves the fracture toughness.

More investigations are in progress to confirm this behavior. For this purpose, we are using Digital Image correlation DIC to study the local displacement field around the crack tip.

7. Conclusion

The 3D printing by Fused Depositing Modeling uses currently a classical trajectory in order to deposit a thread layer by layer. The research approach reproduces the principal stress directions from finite element simulation inside the internal structure of samples realized in extrusion deposition by 3D printing for improve the fracture toughness. The depositing follows the principal directions with alternate layers and a trajectory which draws the same stress fields. The alternate layers are lead manually into the G-code language in order to replicate the two directions. The mechanical characterization in fracture shows that the optimized C-T samples are strengthened up to 20% compared to classical samples. Currently, 2D Digital Image Correlation (DIC) is used to study the deformation mapping to compare the results with the numerical simulation and will be presented in a next paper.

The samples are currently realized on 2D sections with a projection of stress fields on the 3D model and we can propose in perspective a spatial representation in 3D with an internal structure able to resist to mechanical applied stress. Others mechanical characterizations are ongoing to reinforce the results in order to tend to a numerical model. A take into account of the mixed mode loading associated to specific reinforced specimens will be done on the basis of results issued from reference (Li et al., 2004).

References

Abramovitch, H., Burgard, M., Edery-Azulay, L., Evans, K.E., Hoffmeister, M., Miller, W., Scarpa, F., et al. (2010), “Smart tetrachiral and hexachiral honeycomb: Sensing and impact detection”, *Composites Science and Technology*, Vol. 70 No. 7, pp. 1072–1079.

Ahn, S.-H., Montero, M., Odell, D., Roundy, S. and Wright, P.K. (2002), “Anisotropic material properties of fused deposition modeling ABS”, *Rapid Prototyping Journal*, Vol. 8 No. 4, pp. 248–257.

Beaman, J.J., Barlow, J.W., Bourell, D.L., Crawford, R.H., Marcus, H.L. and McAlea, K.P. (1997), “Solid freeform fabrication: a new direction in manufacturing”, *Kluwer Academic Publishers, Norwell, MA*, Vol. 2061, pp. 25–49.

Crump, S.S. (1992), *Apparatus and Method for Creating Three-Dimensional Objects*, Google Patents, available at: http://www.google.com/patents/US5121329 (accessed 17 December 2014).

Crump, S.S. (1994), *Modeling Apparatus for Three-Dimensional Objects*, Google Patents, available at: http://www.google.com/patents/US5340433 (accessed 17 December 2014).

Galantucci, L.M., Lavecchia, F. and Percoco, G. (2008), “Study of compression properties of topologically optimized FDM made structured parts”, *CIRP Annals - Manufacturing Technology*, Vol. 57 No. 1, pp. 243–246.

Gardan, J. (2015), “Additive manufacturing technologies: state of the art and trends”, *International Journal of Production Research*, Vol. 0 No. 0, pp. 1–15.

Li, J., Zhang, X.-B. and Recho, N. (2004), “J–M p based criteria for bifurcation assessment of a crack in elastic–plastic materials under mixed mode I–II loading”, *Engineering Fracture Mechanics*, Vol. 71 No. 3, pp. 329–343.

Malone, E. and Lipson, H. (2007), “Fab@Home : the personal desktop fabricator kit.”, *Mechanical and Aerospace Engineering, Cornell University, Rapid Prototyping Journal*, Vol. Emerald Group Publishing.

Miller, W., Smith, C.W., Scarpa, F. and Evans, K.E. (2010), “Flatwise buckling optimization of hexachiral and tetrachiral honeycombs”, *Composites Science and Technology*, Vol. 70 No. 7, pp. 1049–1056.

Prall, D. and Lakes, R.S. (1997), “Properties of a chiral honeycomb with a Poisson’s ratio of—1”, *International Journal of Mechanical Sciences*, Vol. 39 No. 3, pp. 305–314.

Vesenjak, M., Krstulović-Opara, L., Ren, Z. and Domazet, Ž. (2010), “Cell shape effect evaluation of polyamide cellular structures”, *Polymer Testing*, Vol. 29 No. 8, pp. 991–994.